

# Circular Polarization for L-band Radiometric Soil Moisture Retrieval

Roger D. De Roo, Anthony W. England  
Department of Atmospheric, Oceanic and Space Sciences  
The University of Michigan  
2455 Hayward Street  
Ann Arbor, MI 48109-2143, USA  
+1 (734) 647-8779  
deroo@umich.edu

Jiyoun Munn  
EMAG Technologies, Inc.  
1340 Eisenhower Place  
Ann Arbor, MI 48108, USA  
+1 (734) 973-6600

*Abstract*— For microwave radiometric retrievals of surface soil moisture at L-band, the preferred polarization is horizontal polarization, because it has higher sensitivity to the soil moisture than does vertical polarization. However, L-band observations of the Earth's surface from space may experience significant Faraday rotation. We describe the consequences of using circular polarization to L-band Synthetic Thinned Array Radiometer (STAR) observations of soil moisture. While sensitivity to soil moisture is somewhat reduced, the sensitivity to Faraday rotation is eliminated. Circular polarization also presents the engineering advantage of requiring only one type of receiver/antenna pair in a 2-D STAR, instead of three for any linear polarization. We present a sensitivity analysis and a derivation of the design requirements for a circularly polarized antenna for use in a STAR. An implementation of the antenna for an airborne system, STAR-Light, is also presented.

## TABLE OF CONTENTS

- 1 INTRODUCTION
- 2 CHARACTERISTICS OF CIRCULAR POLARIZATION FOR SOIL MOISTURE RETRIEVAL
- 3 CIRCULAR POLARIZATION FOR A 2-D STAR CONFIGURATION
- 4 DESIGN REQUIREMENTS FOR STAR-LIGHT
- 5 STAR-LIGHT ANTENNA IMPLEMENTATION
- 6 CONCLUSIONS
- 7 ACKNOWLEDGMENTS

## 1. INTRODUCTION

Soil moisture is a critical parameter for modeling the near term weather and regional climate [1]. L-band microwave radiometry is the technique with perhaps the greatest sensitivity to the surface soil moisture signal while retaining the

least sensitivity to unmeasurable interfering signals, like vegetation [2]. As a result, technology is being pushed toward the launch of L-band radiometers for remote sensing of soil moisture. However, the desired spatial resolution is that of a storm track, typically 10 km. At the long microwave wavelength of 21 cm, this resolution requires apertures 15 m in diameter from low Earth orbit. At this size, alternative instrument architectures to traditional scanning reflectors have strong appeal. Perhaps the strongest candidate architecture to achieve this size is Synthetic Thinned Array Radiometry (STAR) [3].

The European Space Agency (ESA) is employing 2-D STAR technology for the Soil Moisture and Ocean Salinity (SMOS) mission [4]. SMOS has three legs each 4.5 m long, resulting in a spatial resolution as sharp as 30 km. SMOS has advanced to phase C/D development and has a current launch date of February 2007.

Horizontal polarization is preferred for its greater sensitivity to soil moisture when compared to vertical polarization. L-band horizontal polarization brightness sports a sensitivity of about  $dT_H/dm_v = -3 \text{ K}/\%$  to  $-5 \text{ K}/\%$  at an incidence angle of  $55^\circ$ , depending on the value of the volumetric moisture  $m_v$ , while vertical polarization at the same angle has a sensitivity of about  $dT_V/dm_v = -2 \text{ K}/\%$ . However, at 1.4 GHz, Faraday rotation on transmission through the atmosphere can result in significant changes in the polarization state between the signal that is emitted at ground level and the sensor in orbit [5]. Some proposed solutions to this problem include estimating the effects by making multiple polarization or polarimetric measurements [6] or by making H-polarized measurements at restricted altitudes, incidence angles, and times of day so that the errors generated by Faraday rotation are minimized [7].

One possible solution to the problem of Faraday rotation which does not require multiple polarization measurements or knowledge of Faraday rotation characteristics is to employ circularly polarized antennas for the radiometer. This ap-

proach is being employed by the authors for the STAR-Light instrument, a small, 10-element 2-D STAR to be mounted on a light aircraft for the purpose of validating soil-vegetation-atmosphere-transfer (SVAT) models of the Arctic [8]. We describe the consequences of the use of circular polarization on the sensitivity of the instrument in section 2. An engineering advantage to circularly polarized antennas over linearly polarized antennas for use in 2-D STARs is described in section 3. Specific design requirements for the application of circularly polarized antennas in the STAR-Light instrument are described in section 4. Despite the fact that these antennas were intended for a specific instrument, the design requirements for STAR instruments bear many similarities. Finally, in section 5 we describe the implementation of the requirements in the production of a pair of prototype STAR-Light antennas.

## 2. CHARACTERISTICS OF CIRCULAR POLARIZATION FOR SOIL MOISTURE RETRIEVAL

Circular polarization at 1.4 GHz has the distinct advantage over linear polarizations in transmissions through the atmosphere in that the signals are less susceptible to the distorting effects of Faraday rotation. Circular polarization is less sensitive to the soil moisture signal, however, and the benefits of the elimination of Faraday rotation must be weighed against the loss of sensitivity.

### *Sensitivity to Soil Moisture*

At microwave frequencies less than about 9 GHz, the dielectric constant of liquid water is much higher than most other materials found in nature. Below 1 GHz, the sky is no longer cold, as the galactic contribution can be quite large [9]. As a result, in this frequency range, microwave brightness of bare, flat soil exhibits a direct dependence on its temperature, and an inverse relationship on its moisture. Moreover, the long 21 cm wavelength at the 1.4 GHz radio astronomy window provides for significant penetration of vegetation [10] and decreases the normalized surface roughness. Ulaby *et al.* [11] describe at length the quantitative features of passive remote sensing of soil moisture at 1.4 GHz. For illustration, Figure 1 shows the brightness vs. incidence angle as observed by a linearly polarized 1.4 GHz radiometer when looking at a smooth specular bare soil at a physical temperature of 300 K and different soil moistures. Except for the motion of the Brewster angle toward grazing, increasing moisture manifests itself as a decrease in the brightness. Horizontal polarization clearly exhibits a greater sensitivity to soil moisture regardless of incidence angle, and this is why it is preferred over vertical polarization for this observation.

The circularly polarized brightness for the same three conditions of moisture for bare soil can be seen in Figure 2. The

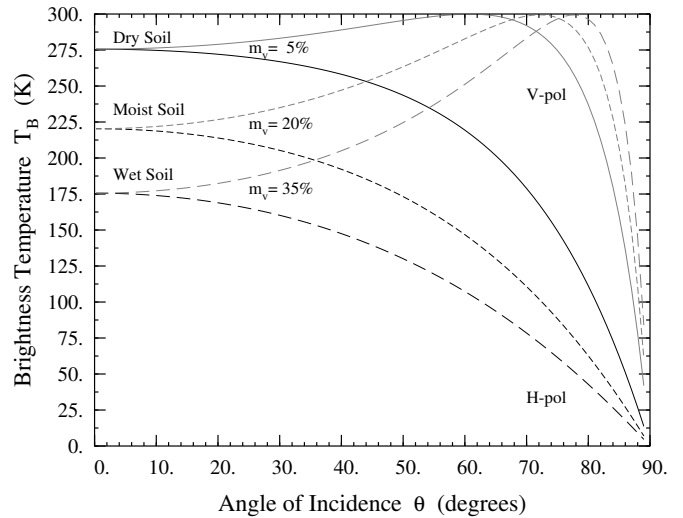


**Figure 1.** Linearly polarized brightness temperatures for bare specular soil at a physical temperature of 300 K.

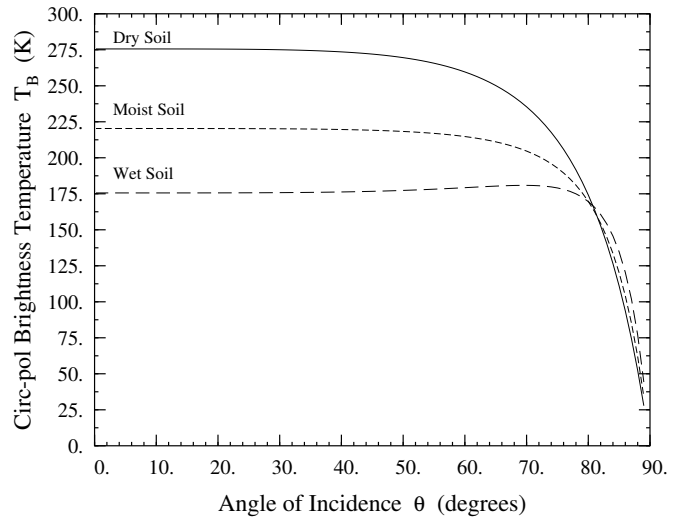


**Figure 2.** Circularly polarized brightness temperatures for bare specular soil at a physical temperature of 300 K.

brightness values in this figure are valid for both left circular polarization (LCP) and right circular polarization (RCP), and in fact is the arithmetic mean of vertical and horizontal brightnesses. This is because vertical polarization can be decomposed into equal amplitude and in-phase left and right circular polarized components, while horizontal polarization can be decomposed into equal amplitude but opposite phase left and right circular polarized components, and the vertical and horizontal components are assumed to be uncorrelated. The main features of the circular polarization brightness dependence on soil moisture is that the brightness is nearly constant for angles from nadir out to nearly 60°. Beyond that angle, however, the sensitivity to soil moisture decreases rapidly.

The sensitivities of the radiometric signal to soil moisture are

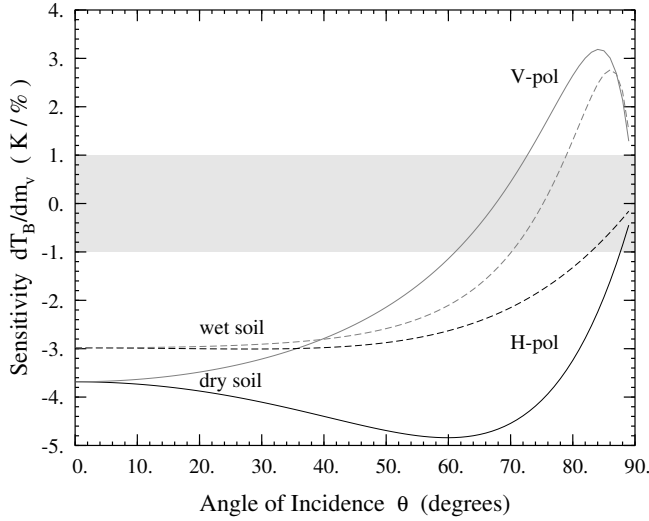


**Figure 3.** Linearly polarized sensitivity for the bare specular soil of Figures 1 and 2.

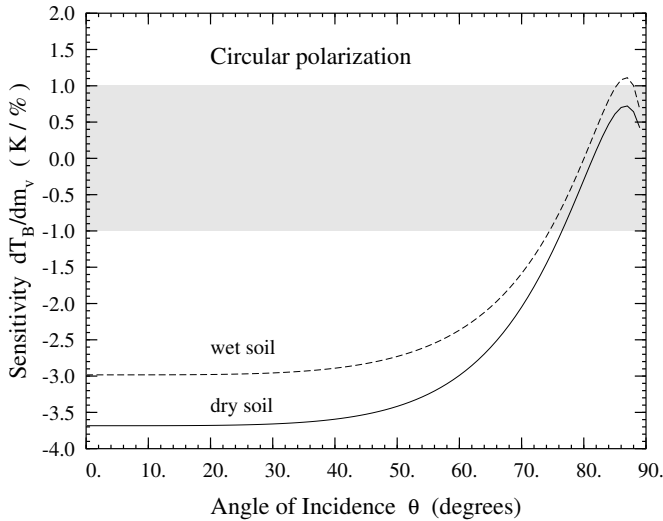


**Figure 4.** Circularly polarized sensitivity for the bare specular soil of Figures 1 and 2.

shown in Figure 3 for linear polarizations and in Figure 4 for circular polarization. The curves in these figures simply represent the differences in brightness of the curves in Figures 1 and 2, normalized by the 15% volumetric moisture differences. The regions of less than 1 K/% sensitivity, where other factors such as vegetation and surface roughness could overwhelm the soil moisture signal, are shown in gray. This level of corruption by factors beyond the control of the instrument designers also determines the required instrument sensitivity of 0.5 K. While  $H$ -polarization shows the greatest sensitivity overall, the sensitivity of circular polarization is adequate to angles as far as  $70^\circ$  from nadir.

### Faraday rotation

Faraday rotation is an artifact of propagation of the signal wave through the ionospheric plasma in the presence of the Earth's static magnetic field. The plane of oscillation of a linearly polarized electric field is rotated by  $\phi$  radians, where

$$\phi = \frac{q^3 \eta}{2m_e^2 \omega^2} \int N_e \mathbf{B} \cdot d\mathbf{s} \quad (1)$$

$\omega = 2\pi f$  is the angular frequency, in radians/s,  $N_e$  is the plasma density, in electrons/m<sup>3</sup>,  $q = 0.1602$  aC is the magnitude of the charge of the electron, the charge to mass ratio of the electron is  $q/m_e = 176$  C/ $\mu\text{g}$ ,  $\eta = 377$   $\Omega$  is the intrinsic impedance of free space,  $\mathbf{B}$  is the Earth's magnetic field, and  $d\mathbf{s}$  is an incremental path along the direction of propagation. The change in the plasma density  $N_e$  is fairly large and unpredictable over the course of a day. In part because the plasma density is often at a daily minimum at dawn, most L-band radiometry missions are proposed for sun synchronous orbits with 6 AM local observation times.

LeVine and Kao [7] analyzed the errors introduced by Faraday rotation on an orbiting  $H$ -polarized L-band instrument. The relative error in brightness is given by

$$\frac{\Delta T_B}{T_B} = (1 - \epsilon_V / \epsilon_H) \sin^2 \phi \quad (2)$$

where  $\epsilon_V$  and  $\epsilon_H$  represent the surface emissivity for  $V$ - and  $H$ -polarizations. They found that most days near dawn, the expected errors  $\Delta T_B$  were acceptable (less than 1 K) for angles less than  $40^\circ$ , but increased rapidly for larger angles. This is because the difference in emissivity between  $V$ - and  $H$ -polarizations increases rapidly with incidence angle.

Extending the above analysis to a system with elliptical polarized antennas with an axial ratio of  $AR$ , in dB, and oriented with the major axis to coincide with horizontal, the above expression becomes

$$\frac{\Delta T_B}{T_B} = \frac{1 - 10^{-AR/10}}{1 + 10^{-AR/10}} (1 - \epsilon_V / \epsilon_H) \sin^2 \phi \quad (3)$$

which reduces to the above expression for an infinite axial ratio. For a perfectly circularly polarized antenna, for which  $AR = 0$  dB, the error due to Faraday rotation is zero. Even for a system with an  $AR = 3$  dB, the error is reduced to one third that of an  $H$ -polarized system under the same conditions.

For circular polarization, Faraday rotation manifests itself as a phase shift of  $\phi$ , akin to a small, diffuse permittivity change. As such, the polarization state is not disturbed, but it is not possible to construct a polarimetric system (dual polarized with relative phase measurements) from a circular basis, since reconstruction of the polarizations prior to Faraday rotation is

next to hopeless (the phase shift is in opposite senses for left and right circular polarization). Fortunately, a space-borne circularly polarized L-band radiometer would need only one circular polarization, not both.

A broad field of view STAR system will view the scene through many angles of incidence, possibly different electron densities, and even over different portions of the Earth’s magnetic field. Nonetheless, while the scene may not be viewed through a constant Faraday rotation angle, STAR systems will still work since each portion of the scene contributing signal to an antenna pair (ie. visibility) experiences the same Faraday rotation. Thus, L-band STAR systems employed for soil moisture monitoring from space will not be subject to errors due to Faraday rotation if a single circular polarization is chosen for reception, regardless of the angle of incidence.

### 3. CIRCULAR POLARIZATION FOR A 2-D STAR CONFIGURATION

Near nadir, the distinction between  $V$  and  $H$  polarizations is academic. As a result, for a near-nadir viewing instrument, such as STAR-Light, there is no loss of sensitivity in the choice to use circular polarization. Likewise, at the relatively low altitudes of a light aircraft, the platform for STAR-Light, the Faraday rotation is negligible. However, circular polarization has a distinct engineering advantage for the two-dimensional STAR configuration that STAR-Light has adopted.

The optimal layout for a 2-D STAR is with the antennas forming a three legged array, with legs  $120^\circ$  apart and the same number of antennas on each leg, as depicted in Figure 5. This Y-shaped array appears to be optimal in the sense that it produces the most distinct visibilities for a given number of antennas [12]. Also, the positioning of the antennas on a hexagonal grid produces a slightly larger inter-element spacing requirement than for a rectangular array. The maximum angle from boresight for an alias-free field of view,  $\theta_{AFFOV}$ , can be found from

$$\sin \theta_{AFFOV} = \frac{2\lambda}{\sqrt{3}d} - 1 \quad (4)$$

resulting in a requirement for antenna spacing,  $d$ , between  $0.577\lambda$ , where the alias-free field of view extends across the entire field of view, and  $1.155\lambda$ , where the alias-free field of view has shrunk to nothing. A margin must be included in the antenna spacing to account for the aliasing of the impulse response of the array. Even with this spacing advantage over rectangular arrays, the spacing between antennas for an Earth-looking array is quite tight. Also, the antennas must be physically close to their receivers, so as to minimize signal to noise degradation in the transmission line between them.

With the tight spacing and requirement for close proximity to

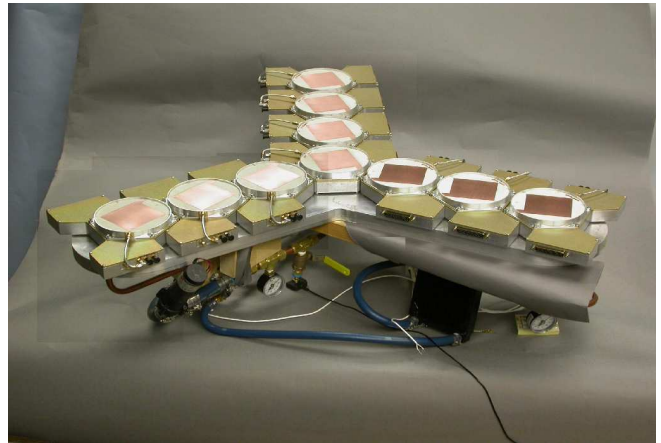


**Figure 5.** A photo mosaic depicting the Y-array layout of the 10 receivers for STAR-Light mounted on a thermal control system. The image is a composite of several photographs of the two prototype STAR-Light receivers.

the antennas, a specialized shape was adopted for the STAR-Light receiver. This enabled the antenna/receiver pairs to be configured in the optimal Y-array shape with a spacing as close as  $0.683\lambda$ , as shown in Figure 5. The drawback to this configuration is that the receivers are now oriented in three different directions, one orientation for each leg. Linearly polarized antennas attached to these receivers, in order for them all to be co-aligned, must conform to one of the following two undesirable designs: The antennas must be attached through potentially long cables reaching around from the antenna port to the receiver on one or more legs, which would imply noisy reception on those legs. Alternatively, the antennas or receivers must be designed differently for each leg to maintain short leads, which is expensive. Also, the STAR-Light design called for interchangeable antenna/receiver pairs, to facilitate field-maintainability, which is complicated by separate designs for the antenna/receivers on each leg.

Circularly polarized antennas enable a single unified design for the antenna/receivers to be mounted in different orientations while maintaining a polarization match between the antennas in the array. Figure 6 depicts the three circularly polarized antenna orientations for the STAR-Light array. The different orientations appear in the image processing algorithm for the STAR as different multiples of  $120^\circ$  phase shifts. Because of this advantage, circularly polarized antennas were specified for STAR-Light.

### 4. DESIGN REQUIREMENTS FOR STAR-LIGHT

While STAR-Light was specified to implement circularly polarized antennas for the simplicity provided by a unified array design, antennas for STAR systems must meet a number of performance parameters for satisfactory STAR performance. These parameters include the bandwidth, gain, gain ripple,



**Figure 6.** A close-up of the previous Figure, showing the three orientations of the receivers, with one orientation per leg. Each antenna has a fixed orientation with respect to its receiver. Since each antenna is left circularly polarized, rather than linearly polarized, the polarization states remain aligned regardless of antenna orientation.

VSWR and radiation efficiency. For the implementation of the circularly polarized antennas in STAR-Light, additional requirements must be met with regard to the axial ratio and the azimuthal symmetry of the gain and axial ratio.

#### Requirements imposed by 2-D STAR

**Bandwidth**—The bandwidth of the entire STAR system is established by the radioastronomy window from 1400 to 1427 MHz. In this window, transmitters are forbidden, which enables radiometric observations to take place without interference. Significant interfering signals are expected immediately outside of this band, and requirements are imposed on the receiver to prevent these signals from interfering with the radiometric observations. By identifying the commercially available ceramic filter which produced the widest pass band while achieving appropriate out of band rejection and sufficiently small insertion loss, it was determined that the receiver design, and therefore the following antenna design requirements, must be met over a 21 MHz bandwidth centered at 1413.5 MHz.

**Gain envelope**—With the array spacing fixed at  $0.683\lambda$ , the alias-free field of view extends from nadir out to  $35^\circ$ . Within this field of view, the antenna gain must remain high to keep the instrument sensitive to the scene under observation. Outside of the field of view, aliases of the scene from near the horizon appear close to the opposite edge of the field of view. To keep these aliases sufficiently small, the gain toward the horizon must be sufficiently small for each individual antenna in the array. Trade-off studies on gain envelope shape results in the normalized gain envelope shown in Figure 7.

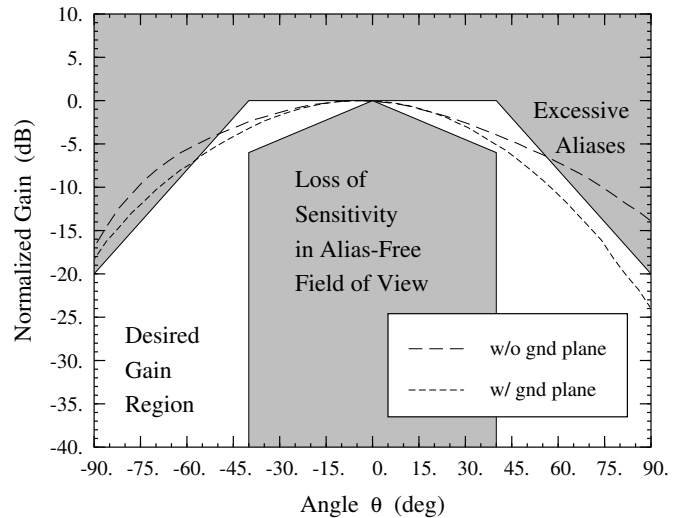


**Figure 7.** STAR-Light antenna gain envelope, and preliminary test results. The gain is normalized to maximum gain. The wide impulse response of the small STAR-Light array places a burden on the individual antennas to reduce unwanted aliases outside of the field of view.

Of all the antenna parameters described in this section, the gain envelope is likely the most dependent on the details of the instrument implementation. Larger arrays, smaller inter-element spacing, smaller instrument field of view, and a higher operational altitude will each relax the requirements on the antenna element gain roll-off near the horizon. Larger arrays produce a tighter array impulse response, resulting in less bleeding of the aliases into the field of view. Smaller inter-element spacing pushes the aliases away from boresight by increasing the size of the alias-free field of view. Conversely, a smaller instrument field of view relaxes the roll-off requirement by moving the area of interest away from the contaminating aliases. Finally, operations from low earth orbit help by removing the warm sources at the instrument horizon which generate the aliases.

**Gain ripple**—Camps *et al.* [13] provide a brief analysis of the impact of antenna gain and phase ripple on the fidelity of image generation. Applying their approach to the STAR-Light system, a requirement of 0.3 dB maximum ripple in magnitude and  $3^\circ$  maximum ripple in phase in the gain pattern was established.

**VSWR**—A small return loss looking into the antenna is important for reducing self-interference of noise generated within the receiver with that same noise reflected back into the receiver from the antenna. Temperature changes or mechanical loading changes can change the relative phasing of these two signals, changing the amount noise being generated in the receiver outside the points of injection of calibration signals. A good VSWR also is indicative of good coupling of

the free space signal into the receiver. A return loss of -23 dB (VSWR=1.15:1) was specified to keep this reflected signal level to 1.5 K. Phase changes due to thermal or mechanical changes are expected to be significantly less than  $\lambda/2$ , reducing this uncompensated error term to negligible levels.

*Radiation efficiency*—The radiation efficiency quantifies the noise figure of the antenna as employed in a radiometer. A budget was developed to assign allowable noise figures for the antenna, radome, transmission line, and receiver front end for satisfactory performance of the receiver as a whole. In this budget, a loss of 0.36 dB was assigned to the antenna. This corresponds to a radiation efficiency of 92%.

*Mutual Coupling*—Coupling between antennas in the STAR array results in a low level of correlated noise in those antennas. This correlated noise is generated within the front end of a receiver, and is therefore present at both the receiver generating the noise and at another receiver through mutual coupling of the antennas. This correlated noise manifests itself in the STAR processing as a scene independent offset to the visibility. It would be highly desirable to limit this offset to negligible levels by requiring low mutual coupling, but this results in a requirement of the order of -40 dB, which would allow 0.03 K of noise coupling from a receiver generating 300 K of noise from its front end isolator. While a realistic objective for non-adjacent antennas, this level of mutual coupling is unrealistic for adjacent antennas. The design objective for the STAR-Light antennas was simply to keep this adjacent antenna mutual coupling as small as was reasonably possible, with a goal of -28 dB (1 K of coupled noise). The instrument calibration procedure must be sufficient to quantify the level of coupling in each adjacent antenna pair. The fact that there are several redundant adjacent pairs of antennas in the STAR array may help the task of instrument calibration on this regard.

#### Circular Polarization Requirements

*Axial Ratio*—The usual specification for circularly polarized antennas is the Axial Ratio, abbreviated AR, defined as the ratio of the major axis to minor axis of the polarization ellipse and usually given in dB. A given polarization state may be described by a Jones vector:

$$\mathbf{p} = \frac{1}{\sqrt{|v|^2 + |h|^2}} \begin{pmatrix} v \\ h \end{pmatrix} \quad (5)$$

For an ideal left-hand circularly polarized wave,  $v = 1$  and  $h = j$ . For a wave with an axial ratio  $AR$  given in dB, and major axis in the  $\hat{v}$  direction, we would use  $v_1 = 10^{AR/20}$  and  $h_1 = j$ . For another antenna which satisfies the same axial ratio specification, the most different polarization state would be one with the major axis in the  $\hat{h}$  direction:  $v_2 = 1$

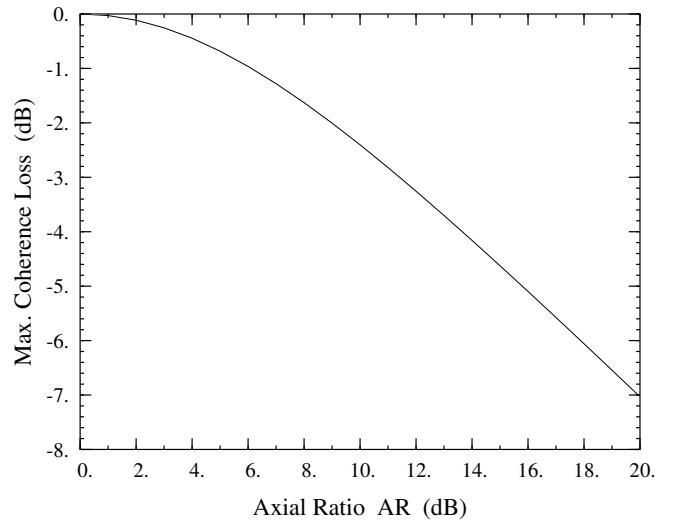


**Figure 8.** Worst case coherence loss due to polarization mismatch for circularly polarized antennas used in a STAR.

and  $h_2 = j10^{AR/20}$ .

These two antennas would be the worst case for two circularly polarized antennas which still met the specification for a given  $AR$ . The reduction in the coherence of the signal seen between these two antennas due to polarization mismatch is given by

$$\mathbf{p}_1^\dagger \cdot \mathbf{p}_2 = \frac{2 \cdot 10^{AR/20}}{1 + 10^{AR/10}} \quad (6)$$

where  $\mathbf{a}^\dagger$  is the Hermitian conjugate of the vector  $\mathbf{a}$ .

The maximum loss of coherence due to polarization mismatch for two antennas which each satisfy the axial ratio specification  $AR$ , according to Equation 6 is shown in Figure 8.

In particular, the maximum coherence loss for an axial ratio of 3 dB (the specification for STAR-Light) is 0.942, or -0.26 dB.

*Azimuthal Symmetry*—Since these antennas will be mounted in the array in three orientations, one on each STAR leg, the antennas must behave sufficiently like each other in each of those three positions. The rotational repeatability need not be all the way from nadir to the horizon, however, but only over the field of view (with a little margin). Together, these constitute a 3-way symmetry requirement from nadir out to  $40^\circ$ . The symmetry requirements manifest themselves in two aspects: axial ratio and gain. Analysis similar to that for the axial ratio above yields requirements of axial ratio repeatability of 3 dB peak to peak. Gain repeatability between antennas is considerably tighter at 1.5 dB peak to peak.

*Polarization State*—The choice of polarization state, that is, left circular or right circular, is of no consequence to the science requirements of the instrument. However, appropriate choice of one of these two may assist in interference rejection for anthropogenic signals generated near the radio astronomy band. Such interference would be most problematic when looking at very cold targets. The coldest such target is the sky, which is intended to be used as part of the instrument calibration procedure. As such, the polarization should be chosen to mismatch any circularly polarized downlink from a satellite that uses a nearby frequency. The left circular polarization requirement was chosen to minimize the possible interference from the INMARSAT system, with a right circular polarization downlink at 1525 to 1559 MHz <sup>1</sup>.

## 5. STAR-LIGHT ANTENNA IMPLEMENTATION

We approached the task of designing an antenna to meet this difficult set of requirements by prioritizing the objectives. The frequency and radiation efficiency requirements were both such that failure to meet them results in an instrument which was susceptible to errors that were not correctable. Thus, these requirements were given the highest priority. Failure to meet gain envelopes and axial ratio requirements results in an instrument with reduced sensitivity in certain portions of the field of view, and so these were given a high, but not the highest, priority. It is possible to model the VSWR and mutual coupling behavior of the antenna in the calibration algorithm, and so these requirements were given a lower priority.

A machined aluminum cup was designed to facilitate the mechanical fastening of the antenna to the receiver. To achieve a high radiation efficiency, we designed a patch antenna on Rogers 4003 Duroid 20 mils thick suspended within the metal cup to achieve an air gap of 0.3 inches between the Duroid and the base of the cup. The patch itself is a corner fed rectangular patch, with the sides tuned to frequencies just above and below the center frequency of 1413.5 MHz [14]. Tuning tabs are attached to both the patch itself and to the microstrip feed. Two prototypes are shown in Figure 9.

Preliminary measurements on these prototypes have been conducted. Gain measurements, shown in Figure 7 with the gain envelope, indicate that sufficient gain is attained within the antenna field of view (nadir to 40°), but that in a few azimuthal directions the gain is only down by 15 dB. This will cause aliasing errors at some edges of the instrument field of view, and may result in a narrowing of the useful instrument field of view. Some measurements in the presence of an extended ground plane indicate that this is important to achieving the intended roll-off in gain near the antenna horizon, as shown in the figure. The gain ripple requirements are satis-



**Figure 9.** STAR-Light prototype antennas employ corner-fed microstrip patches on a suspended substrate for left circular polarization.

fied across the instrument field of view. The antenna VSWR is less than 1.13 across the pass band, and is in fact, better than 1.10 over most of it. The radiation efficiency has not yet been measured; this measurement is awaiting integration with the prototype STAR-Light receivers. Mutual coupling for adjacent antennas is measured at  $-27$  dB, missing the objective by only 1 dB. Mutual coupling for non-adjacent antennas has not yet been measured. The axial ratio measurements indicate excellent performance across the field of view, with few departures from the requirement. The azimuthal symmetry analysis is ongoing.

## 6. CONCLUSIONS

Circular polarization presents some advantages for radiometric Earth remote sensing at lower microwave frequencies. The loss of sensitivity to soil moisture by using circular polarization instead of the most sensitive horizontal polarization is minimal near nadir, and is significant only for incidence angles beyond 60°. The major advantage to the choice of circular polarization is the reduction of the instrument sensitivity to the effects of Faraday rotation in the Earth's ionosphere.

Circularly polarized antennas also have the potential to simplify the construction of two dimensional synthetic thinned array radiometers (2-D STAR). The optimal shape of such an array has three legs 120° apart. Implementation of a single design linear or dual linear polarized antenna into this architecture can be awkward. Properly designed circularly polarized antennas can be implemented on any leg of a 2-D STAR without disruption to the sensitivity of the instrument. The requirements for such a circularly polarized antenna for a small 2-D STAR are described, and the results of a prototype antenna constructed for this instrument are presented. The requirements are severe, but an antenna can be manufactured that satisfies them.

<sup>1</sup><http://www.seaveyantenna.com/catalog/p14/pg14.htm>

## 7. ACKNOWLEDGMENTS

This work is supported by National Science Foundation grant OPP-0085176 from the Office of Polar Programs. The authors wish to thank Panayotis Frantzis and Karl Brakora, whose assistance in the design, fabrication and testing of the prototype antennas is greatly appreciated.

## REFERENCES

- [1] D. Entekhabi, G. R. Asrar, A. K. Betts, K. J. Beven, R. L. Bras, C. J. Duffy, T. Dunne, R. D. Koster, D. P. Lettenmaier, D. B. McLaughlin, W. J. Shuttleworth, M. T. van Genuchten, M.-Y. Wei, and E. F. Wood, "An agenda for land surface hydrology research and a call for the second international hydrological decade," *Bulletin of the American Meteorological Society*, vol. 80, pp. 2043–2058, Oct. 1999.
- [2] T. J. Jackson and T. J. Schmugge, "Passive microwave remote sensing system for soil moisture: Some supporting research," *IEEE Transactions on Geoscience and Remote Sensing*, vol. 27, pp. 225–235, Mar. 1989.
- [3] D. M. Le Vine, "Synthetic aperture radiometer systems," *IEEE Transactions on Microwave Theory and Techniques*, vol. 47, pp. 2228–2236, Dec. 1999.
- [4] Y. H. Kerr, P. Waldteufel, J.-P. Wigneron, J.-M. Martinuzzi, J. Font, and M. Berger, "Soil moisture retrieval from space: The soil moisture and ocean salinity (SMOS) mission," *IEEE Transactions on Geoscience and Remote Sensing*, vol. 39, pp. 1729–1735, Aug. 2001.
- [5] E. J. M. Rignot, "Effect of Faraday rotation on L-band interferometric and polarimetric synthetic-aperture radar data," *IEEE Transactions on Geoscience and Remote Sensing*, vol. 38, pp. 383–390, Jan. 2000.
- [6] S. H. Yueh, "Estimates of Faraday rotation with passive microwave polarimetry for microwave remote sensing of earth surfaces," *IEEE Transactions on Geoscience and Remote Sensing*, vol. 38, pp. 2434–2438, Sept. 2000.
- [7] D. M. Le Vine and M. Kao, "Effects of Faraday rotation on microwave remote sensing from space at L-band," in *Proceedings*, vol. 1 of *IEEE International Geoscience and Remote Sensing Symposium (IGARSS '97)*, pp. 377–379, 1997.
- [8] A. W. England and R. De Roo, "STAR-Light: An enabling technology for modeling Arctic land surface hydrology," in *Proceedings*, IEEE International Geoscience and Remote Sensing Symposium (IGARSS '02), (Toronto, ON), 24–28 June 2002.
- [9] F. T. Ulaby, R. K. Moore, and A. K. Fung, *Microwave Remote Sensing: Active and Passive*, vol. 1. Reading,

MA: Addison-Wesley, 1981.

- [10] B. K. Hornbuckle, A. W. England, M. A. Fischman, R. D. De Roo, and D. L. Boprie, "The influence of a field corn canopy upon the radiometric sensitivity to soil moisture at 1.4 GHz," accepted in *IEEE Transactions on Geoscience and Remote Sensing*, 2003.
- [11] F. T. Ulaby, R. K. Moore, and A. K. Fung, *Microwave Remote Sensing: Active and Passive*, vol. 3. Norwood, MA: Artech House, 1986.
- [12] A. Camps, J. Bará, I. Corbella, and F. Torres, "The processing of hexagonally sampled signals with standard rectangular techniques: Application to aperture synthesis interferometric radiometers," *IEEE Transactions on Geoscience and Remote Sensing*, vol. 35, pp. 183–190, Jan. 1997.
- [13] A. Camps, J. Bará, F. Torres, I. Corbella, and J. Romeu, "Impact of antenna errors on the radiometric accuracy of large aperture synthesis radiometers," *Radio Science*, vol. 32, pp. 657–668, Mar.–Apr. 1997.
- [14] R. C. Johnson, ed., *Antenna Engineering Handbook*. New York: McGraw-Hill, third ed., 1993.



**Roger D. De Roo** (S'88-M'89) received the B.S. in Letters and Engineering degree from Calvin College, Grand Rapids, MI, in 1986, the B.S.E., M.S.E., and Ph.D. degrees from the University of Michigan in 1986, 1989, and 1996 respectively, all in electrical engineering. His dissertation topic was on the model-

ing and measurement of bistatic scattering of electromagnetic waves from rough dielectric surfaces.

From 1996 to 2000, he was employed as a Research Fellow at the Radiation Laboratory in the department of Electrical Engineering and Computer Science (EECS) of the University of Michigan, investigating the modeling and simulation of millimeterwave backscattering phenomenology of terrain at near grazing incidence.

He is employed as an Assistant Research Scientist in the Atmospheric, Oceanic, and Space Sciences department at the University of Michigan. His current research interests include synthetic thinned array radiometer (STAR) technology development and inversion of soil moisture and vegetation parameters from radar and radiometric signatures of terrain.

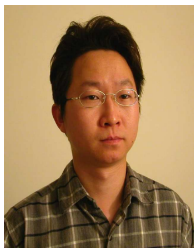


**Anthony W. England** (M'87-SM'89-F'95) received the Ph.D. degree in geophysics from the Massachusetts Institute of Technology, Cambridge, in 1970.

He is Professor of electrical engineering and computer science and Professor of atmospheric, oceanic, and space sciences at the University of Michigan.

His research has included scattering theory applied to the microwave brightness of Earth and planets, and the development and use of ice-sounding radar for the study of glaciers in Alaska and Antarctica. His current research focuses upon developing and calibrating Land-Surface Process/Radiobrightness (LSP/R) models of land-atmosphere energy and moisture fluxes for the North American prairie and the Arctic, and upon developing new radiometer technologies. He has been Co-Investigator for the Apollo 17 Surface Electrical Properties experiment, and Co-Investigator on Shuttle Imaging Radar -A and -C experiments. He was a Scientist-Astronaut during two periods with NASA, where he served as Mission Scientist for Apollo 13 and 16, Mission Specialist on the Spacelab 2 flight in 1985, and Space Station Program Scientist in 1986-1987. He was a Research Geophysicist and Deputy Chief of the Office of Geochemistry and Geophysics with the U.S. Geological Survey from 1972 through 1979, and a Visiting Adjunct Professor at Rice University, Houston, TX, in 1987 before joining the University of Michigan in 1988. He has been an Associate Editor for the *Journal of Geophysical Research*.

Dr. England is a member of the National Research Council's Space Studies Board and chair of several federal committees concerned with science and technology policy. He is a member of the American Geophysical Union.



**Jiyoun Munn** received the B.S. degree in radio sciences and communication engineering from the Hong-Ik University, Seoul, Korea, in 1998, and the M.S. degree in electrical engineering from the University of Michigan, Ann Arbor, in 2000. From 1998 to 2000, he was a Research Assistant in the Radiation Laboratory, at the University of Michigan.

He is currently a Research Engineer at EMAG Technologies, Inc., Ann Arbor, Michigan. His research interests include multi-band antenna design, microwave circuits and radar systems.